EUROPEAN ORGANIZATION FOR NUCLEAR RESEARCH

Proposal to the ISOLDE and Neutron Time-of-Flight Committee

(Following HIE-ISOLDE Letter of Intent I-110)

Mapping single-particle neutron strength towards the mid-shell in semi-magic lead isotopes

January 10, 2024

J. Ojala[1], R. D. Page[1], J. Pakarinen[2,3], M. Alaqeel[4,1], A. N. Andreyev[5], J. Benito[6], P. A. Butler[1], D. J. Clarke[7], J. G. Cubiss[5], A. J. Dolan[1], L. M. Fraile[6] S. J. Freeman[7,8], L. P. Gaffney[1], A. Heinz[9], C. R. Hoffman[10],A. Illana[6], B. R. Jones[1], D. T. Joss[1], B. P. Kay[10], Th. Kröll[11], M. Labiche[12], I. Lazarus[12] , P. T. MacGregor[8], A. Montes Plaza[1,2,3], B. S. Nara Singh[13], P. Papadakis[12], R. Raabe[14], S. Reeve[7], F. A. Rowntree[1], M. Scheck[13], D. K. Sharp[7], J. F. Smith[13], K. Wrzosek-Lipska[15]

[1]*Oliver Lodge Laboratory, University of Liverpool, Liverpool, L69 7ZE, UK*
[2]*Accelerator Laboratory, Department of Physics, University of Jyvaskyla, Jyvaskyla, Finland*
[3]*Helsinki Institute of Physics, University of Helsinki, Helsinki, Finland*
[4]*Imam Mohammad Ibn Saud Islamic University, Riyadh, Saudi Arabia*
[5]*Department of Physics, University of York, York YO10 5DD, UK*
[6]*Grupo de Fisica Nuclear & IPARCOS, Universidad Complutense de Madrid, Madrid, Spain*
[7]*School of Physics and Astronomy, The University of Manchester, Manchester, M13 9PL, UK*
[8]*ISOLDE, CERN, CH-1211 Geneva 23, Switzerland*
[9]*Institutionen för Fysik, Chalmers Tekniska Högskola, S-412 96 Göteborg, Sweden*
[10]*Physics Division, Argonne National Laboratory, Argonne, Illinois 60439, USA*
[11]*Institut für Kernphysik, Technische Universität Darmstadt, D-64289 Darmstadt, Germany*
[12]*STFC Daresbury Laboratory, Daresbury, Warrington, WA4 4AD, UK*
[13]*School of Engineering, University of the West of Scotland, Paisley PA1 2BE, United Kingdom*
[14]*KU Leuven, Institut voor Kern- en Stralinsfysica, 3001 Leuven, Belgium*
[15]*Heavy Ion Laboratory, University of Warsaw, PL-02-093 Warsaw, Poland.*

Spokesperson: Joonas Ojala [joonas.ojala@liverpool.ac.uk], Robert Page [rdp@liverpool.ac.uk], Janne Pakarinen [janne.pakarinen@jyu.fi]
Contact person: Patrick MacGregor [patrick.macgregor@cern.ch]

CERN-INTC-2024-013 / INTC-P-695
10/01/2024

Abstract: We propose to use the ISOLDE Solenoidal Spectrometer to study single-neutron adding reactions on ^{196,198}Pb beams, in order to map the neutron single-particle strength along the Pb ($Z = 82$) isotopic chain. Changing neutron occupancies, most notably of the $\nu 1i_{13/2}$ orbital, have been identified through large-scale Monte-Carlo shell-model calculations as driving the evolution of deformed intruder configurations in this region. The isotopes ^{197,199}Pb were selected for this study because their lowest-lying $\frac{13}{2}^+$ states are clearly separated from other states, allowing the cross sections to be determined unambiguously. The proposed experiment is a first step in a wider campaign envisaged to systematically determine the spectroscopic information necessary for a full understanding of the the underlying shape-driving mechanisms around the neutron mid-shell.

Requested shifts: 26 shifts, (split into 1 run over 1 year)

1 Introduction

The evolution of single-particle structure along isotopic and isotonic chains, moving away from doubly-magic nuclei can explain a myriad of nuclear phenomena, including islands of inversion [1], disappearing shell closures [2] and collective behaviour [3]. Gradual filling of different neutron (proton) orbits changes the magnitude of the interaction with orbitals of the proton (neutron), driving this evolution through the tensor interaction [4]. Recently, this mechanism was invoked to explain the appearance of shape coexistence across the nuclear chart and termed "Type-II" shell evolution [5]. While this description has proved successful in describing neutron excitations across the $N = 40$ shell gap towards ^{68}Ni, describing single-particle occupancies in the neutron-deficient lead isotopes remains an outstanding challenge for modern shell-model calculations [6].

The first large-scale Monte-Carlo shell-model (MCSM) calculations, using a full valence space for protons and neutrons above ^{132}Sn, were performed in the mercury isotopes recently [7]. They showed for the first time that the deformed intruder configurations in this region [8], arising from $\pi(2p-2h)$ and $\pi(4p-4h)$ excitations across the $Z = 82$ shell closure [9], are driven by changes in neutron occupancies; most dramatically of the $\nu 1i_{13/2}$ orbital. In the lead isotopes, large-scale shell-model calculations have been performed using ^{208}Pb as an inert core [10], with a valence space of neutron-hole states in the six orbitals between $N = 82$ and $N = 126$: $\nu 3p_{1/2}$, $\nu 2f_{5/2}$, $\nu 3p_{3/2}$, $\nu 2f_{7/2}$, $\nu 1h_{9/2}$ and $\nu 1i_{13/2}$. Due to the lack of protons in the model space, the deformed intruder configurations were not included, yet good reproduction of experimental energy levels, quadrupole moments and $B(E2)$ values was observed down to ^{196}Pb [11, and references therein]. This implies that the ground states of lead isotopes with $N > 114$ are composed of almost purely spherical neutron configurations and thus provide an excellent testing ground of shell evolution in this region. While part of the challenge remains in the computational complexity of the calculations, the striking lack of spectroscopic information on single-particle states in this region must also be addressed if we are to obtain a full understanding of the underlying mechanism for the shape coexistence observed in lead isotopes around the neutron mid-shell. To address this, we are proposing the first steps towards a systematic study of evolving single-particle strength along the semi-magic lead ($Z = 82$) isotopic chain.

1.1 Physics case

The neutron-deficient lead nuclei have been the subject of intense study into the shape coexistence phenomenon, particularly the characterisation of their excited states [12–16]. The supposed prolate- and oblate-shaped intruder configurations come down in energy approaching the neutron mid-shell at $N = 104$, competing with the near-spherical ground states. This strong competition leads to a triplet of $J^\pi = 0^+$ band-head states at low energy in ^{186}Pb [17]. In the odd-mass lead isotopes, rotational bands built upon the $\frac{13}{2}^+$ isomeric states indicate that this is the band head of an oblate-deformed structure [18, 19], or even a prolate-deformed structure at the mid-shell [20]. Similar structures have been identified in the neighbouring mercury nuclei [21], where the ground states of the odd-mass isotopes display a remarkable jump to large deformations [7]. Coupling of the single $1i_{13/2}$ neutron to the $\pi(2p-2h)$ core lowers this energy of the configuration significantly compared to spherical coupled state [22]. Appreciable $E0$ transitions between excited $\frac{13}{2}^+$ states are observed in ^{195,197}Pb [23, 24] indicating a degree of configuration mixing

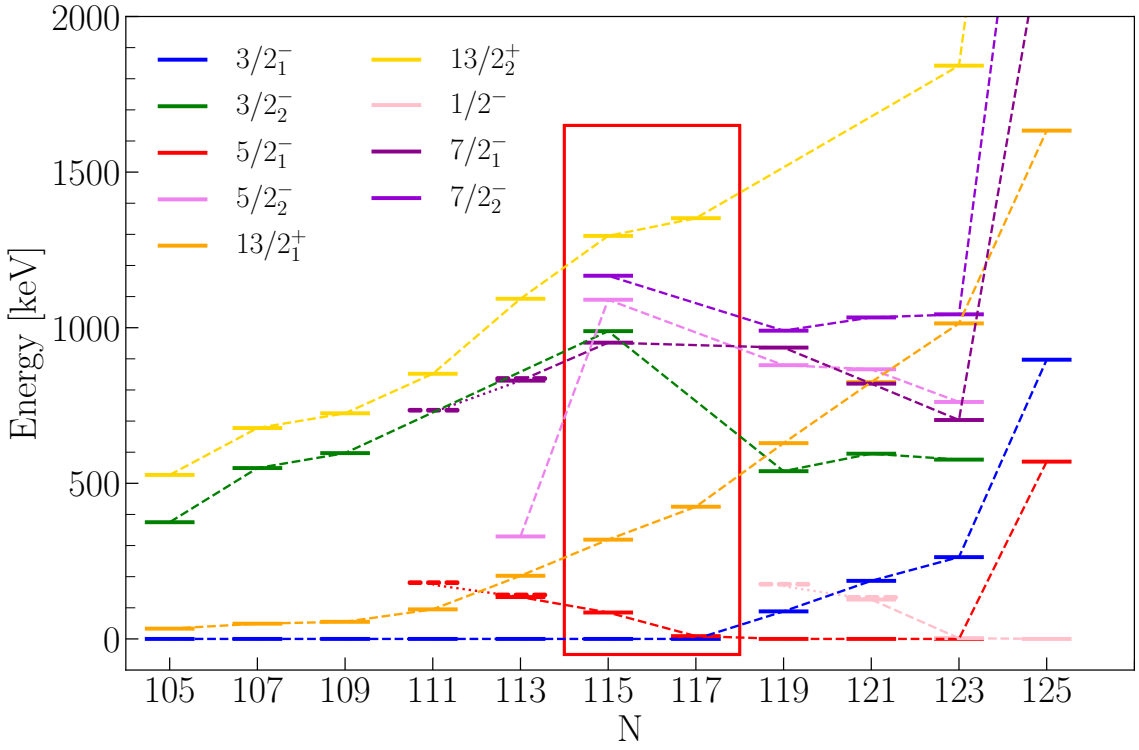

Figure 1: Systematics of energy levels for odd-mass Pb nuclei. Data were obtained from ENSDF. The states of ^{197,199}Pb are shown inside the red box. Note that the low-energy $\frac{13}{2}^+$ isomers in these isotopes are well separated from other states.

is already apparent before reaching the mid-shell [25]. Similar conclusions can be drawn about the observed negative-parity states in these nuclei, originating from the coupling of the $\nu 3p_{3/2}$ with the $\pi(2p-2h)$ intruder configuration, supported by data from α-decay measurements [26].

It becomes crucial then to investigate how the single-particle states evolve down from the $N = 126$ shell closure to the $N = 104$ mid-shell so we could understand the drivers of shape coexistence. The orbitals involved in this region are $\nu 3p_{1/2}$, $\nu 3p_{3/2}$, $\nu 2f_{5/2}$, $\nu 2f_{7/2}$ and $\nu 1i_{13/2}$, which couple to the different core configurations to give rise to $J^\pi = \frac{1}{2}^-$, $\frac{3}{2}^-$, $\frac{5}{2}^-$, $\frac{7}{2}^-$ and $\frac{13}{2}^+$ states in the odd-mass isotopes. The low-lying states obtained mainly in β- and α-decay spectroscopy experiments, which is more sensitive to populating single-particle states than in-beam γ-ray spectroscopy, are shown in Figure 1 for odd-mass lead isotopes. It is noteworthy, that data on single-particle states strongly-coupled to the $\pi(0p-0h)$ configuration are lacking in lead isotopes away from stability. Moreover, there is absolutely no information on how the single-particle strength is distributed.

Objectives: As a route to identify these states and mapping the single-particle strength along the lead ($Z = 82$) isotopic chain, we are proposing to use single-neutron transfer reactions on short-lived ^{196,198}Pb beams to populate excited states in ^{197,199}Pb. The experiment will be performed using the ISOLDE Solenoidal Spectrometer (ISS), which unlike T-REX allows transfer cross sections to be measured for long-lived isomeric states, such as the lowest-lying $\frac{13}{2}^+$ states in ^{197,199}Pb of interest here. These measurements are a first

step in a larger campaign that is planned to systematically approach the mid-shell nuclei in both the Pb and Hg ($Z = 80$) isotopes. It is expected that analysis and interpretation of these data will be completed during LS3, when new proposals will be prepared for the more neutron-deficient isotopes. These new proposals will include the possibility of using odd-mass ground- and isomeric-state beams to probe the configurations of excited states in the even-even isotopes, complementary to Coulomb-excitation experiments performed at Miniball [12, 27, 28].

2 Experiment

2.1 Beam production and yields

Beams of ^{196,198}Pb are required with an energy ≥ 7.5 MeV/u, which have been previously delivered to Miniball at REX energies [12]. The lead beams are produced by bombarding a high-temperature UC_x target with 1.4 GeV proton beam and employing the RILIS laser ion source [29, 30] for ionisation. Yields from the primary target were measured to be $\approx 2\times10^7$ ions/μC. After charge breeding in REX-EBIS and acceleration through the REX and HIE-ISOLDE linacs, a total transmission efficiency of $\epsilon = \epsilon_{EBIS}\cdot\epsilon_{LINAC} = 5\%\cdot70\% = 3.5\%$ can be assumed. Taking an average proton current of 1.5 μA throughout the course of the experiment, the beam intensity at ISS can be expected to be 1.1×10^6 pps. This is consistent with what was observed at Miniball, where the beam purity was measured to be better than 98% [11]. One shift for each isotope will be requested to assess the contributions of ^{196,198}Tl in the beam and measure the beam composition with the laser on/off method for cross-section normalisation.

2.2 Transfer reactions at ISS

The Liverpool on-axis silicon array will be used at ISS to detect the protons emitted from the (d,p) transfer reactions on thin CD_2 targets. The array will be positioned at a distance of 90 mm upstream from the target position. Kinematic calculations for protons from the transfer reaction were performed with a 2.5 T field and 7.5 MeV/u, yielding an angular coverage of the emitted proton ejectiles of between 12° and 47° in the centre of mass frame (see Figure 2). To maximise the detection of protons from the $\ell = 6$ transfer to the $\frac{13}{2}^+$ state, the array is to be positioned as close to the target as possible. A large number of deuterated polyethylene targets, with thicknesses of ≈ 150 μg/cm^2, will be required to compensate for the damage caused by the heavy beams. The newly constructed 2-dimensional target mechanism will be used for this purpose, giving access to more than 50 targets without the need to break vacuum. Depletion of the target material will be monitored using a luminosity monitor placed downstream to detect the elastically scattered deuterons, in combination with a Faraday cup placed behind the target at zero degrees. Additionally, carbon foils will be installed to assess the fusion-evaporation and fusion-fission backgrounds. Potential α-particle background from the decay of fusion products will be subtracted by applying a timing condition on the EBIS pulses, as was done for beams of ^{206}Hg (IS631) [31] and ^{212}Rn (IS689) [32]. Based on PACE4 calculations, 99.5% of the fusion compound nuclei will undergo fission [33], leading to a low background of charged particles on the ISS silicon array. This is supported by experience from the earlier ^{212}Rn experiment (IS689) [32]. Nevertheless, it is important

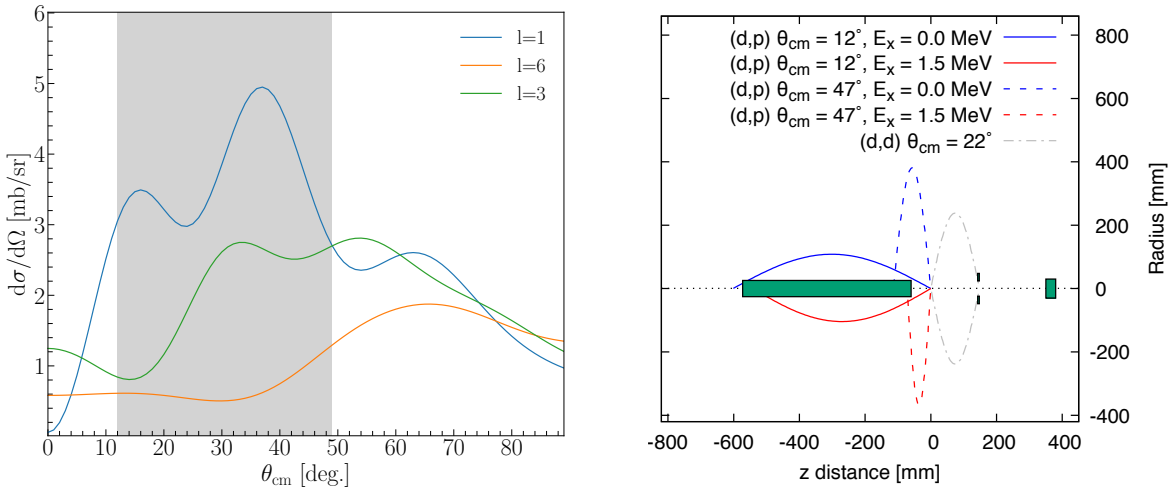

(a) (b)

Figure 2: (a) DWBA calculations for the ^{196}Pb$(d,p)^{197}$Pb reaction at a beam energy of 7.5 MeV/u calculated with Ptolemy (details in main text). The centre-of-mass angular coverage of ISS is indicated by the grey band in the figure. (b) Kinematics for ^{196}Pb$(d,p)^{197}$Pb in inverse kinematics at 7.5 MeV/u using the ISOLDE Solenoidal Spectrometer with a magnetic field strength of 2.5 T.

to measure this background as it can affect the peaks for transfer reactions populating higher-lying states.

Cross sections (see Figure 2 and Table 1) were calculated with Ptolemy [34] using global optical-model parameters determined by Koning and Delaroche [35] for protons and by An and Cai [36] for deuterons. The beam energy used for the simulations was 7.5 MeV/u, corresponding to the maximum beam energy expected for HIE-ISOLDE. A high beam energy is required for the best sensitivity to the angular distributions and to maximise the cross section for the $\ell = 6$ transfer. The angular distributions for $\ell = 1$, $\ell = 3$ and $\ell = 6$ transfer are clearly distinguished. Although this reaction is not sensitive to the different spin-orbit partners, complementary data from α and β decay will be used to confirm the spin of the states populated and distinguish between the population of the $\nu 3p_{1/2}$ and $\nu 3p_{3/2}$ as well as the $\nu 2f_{5/2}$ and $\nu 2f_{7/2}$ single-particle states. The luminosity detector will be placed 180 mm downstream from the target position to obtain an absolute normalisation of the cross sections by measuring the elastically scattered deuterons. This absolute normalisation of the cross sections allows us to extract spectroscopic factors.

The simulation for the proposed experiment was performed using the NPTool framework [37]. The simulated excitation spectrum for ^{197}Pb is shown in Figure 3 as a demonstration of the expected energy resolution 125 keV and peak intensity. Only the low-lying states in ^{197}Pb corresponding to one-neutron transfer to the $\nu 3p_{3/2}$, $\nu 2f_{5/2}$, $\nu 2f_{7/2}$ and $\nu 1i_{13/2}$ orbitals are in these simulations. Fragmentation of the low-ℓ strength across a number of states is expected, due to the mixing of deformed configurations. Although the level scheme for ^{199}Pb is less complete, a similar energy spectrum can be expected, with a cleanly isolated peak arising from transfer to the lowest-lying $\frac{13}{2}^+$ state.

IBM calculations have shown that the ground state 0^+ in ^{196}Pb is dominated at the 98%

Table 1: Calculated reaction cross sections for selected states that may be populated in the ^{196}Pb$(d,p)^{197}$Pb reaction, integrated over the angular coverage of the on-axis silicon array. Also shown are the counts expected per 8-hour shift, assuming an average beam intensity at ISS of 1.1 $\times$ 10^6 pps, a 150 μg/cm^2 target and a geometrical efficiency of $\epsilon_{\rm tot} = \epsilon_\theta \cdot \epsilon_\phi$= 94% $\cdot$ 70% = 66%. The spectroscopic factor is assumed to be $C^2S \approx 0.2$ showing the expected sensitivity level of this experiment.

Energy (keV)	I^π	σ_{DWBA}	Counts per shift
0	$3/2^-_1$	7.8	350
85	$5/2^-_1$	4.5	203
319	$13/2^+_1$	1.4	65
952	$7/2^-_1$	7.7	346
989	$3/2^-_2$	9.4	423
1089	$5/2^-_2$	5.4	243
1167	$7/2^-_2$	8.0	361
1295	$13/2^+_2$	1.6	71

level by the $\pi(0p-0h)$ spherical configuration, with the $\pi(2p-2h)$ oblate contribution at 2% and negligible $\pi(4p-4h)$ prolate content. For this reason, we expect relatively selective transfer to the single-particle states representing coupling of the neutron orbitals of interest with the $\pi(0p-0h)$ spherical configuration. If, for example, the isomeric $\frac{13}{2}^+$ state is the band head of the $\nu 1i_{13/2} \otimes \pi(2p-2h)$ configuration, the $\ell = 6$ transfer strength would be expected to be concentrated predominately in a higher-excited $\frac{13}{2}^+$ state. Alternatively, most authors (e.g., [23, 26]) have interpreted the isomeric $\frac{13}{2}^+$ state in ^{197}Pb as the $\nu 1i_{13/2} \otimes \pi(0p-0h)$ configuration, in which case this state would be more strongly populated. Either way, the *relative cross sections* for transfer to the $\frac{13}{2}^+$ states will directly confirm whether they have underlying intruder or normal configurations for the first time, as well as the degree to which those configurations are mixed in the odd-mass nuclei.

With the achievable energy resolution of 125 keV, the peaks from transfer to the lowest-lying $\frac{13}{2}^+$ states can easily be resolved from the other peaks, which involve $\ell = 1$ and $\ell = 3$ transfers. Although the individual components of these lower-ℓ transfer peaks will not themselves be cleanly resolved, we will be able to fit the cross sections for these multiplets assuming contributions from both ℓ transfers, as was done in Ref. [38]. This analysis will allow us to extract the summed spectroscopic factors for $\ell = 1$ and $\ell = 3$. As mentioned above, complementary decay spectroscopy data from other studies will be used to distinguish the population of the spin-orbit partners and this combined information can then be used to test shell-model calculations. The same fitting methodology can be applied to determine the cross sections for higher-lying $\frac{13}{2}^+$ states if they are not fully resolved from lower-ℓ transfer peaks.

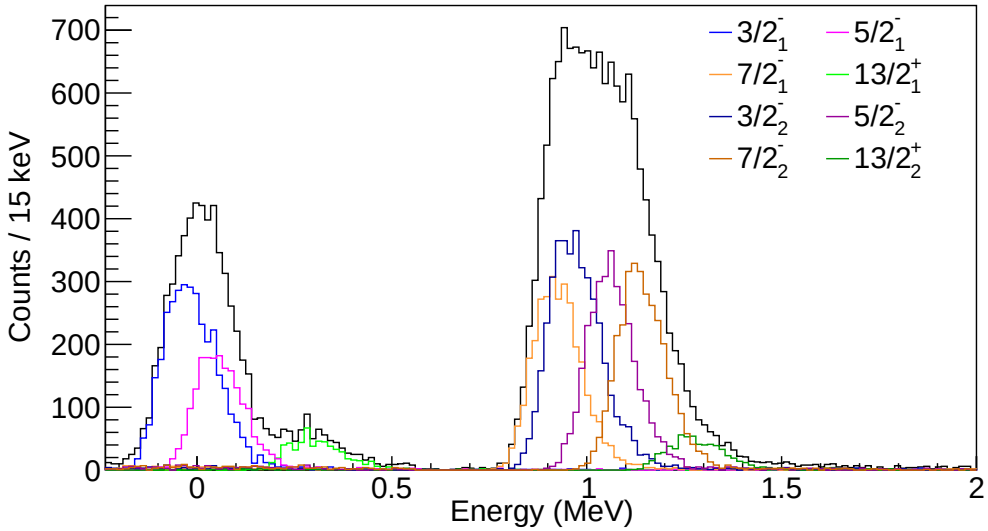

Figure 3: Simulated excitation energy spectra using NPTool for the ^{196}Pb$(d,p)^{197}$Pb reaction taking in to account the expected beam intensity, thickness of the target, magnetic field, angular distribution of emitted protons, the z-position of the array and spectroscopic factors of states which are given in Table 1. The FWHM energy resolution is $\approx$ 125 keV. The component peaks of the fit are indicated by the different colours specified in the key.

Summary of requested shifts: In order to extract spectroscopic factors for the states of interest down to $C^2S \geq 0.2$ and obtain a minimum of 500 counts across the array, 10 shifts each are required for the ^{196,198}Pb$(d,p)^{197,199}$Pb measurements. To measure the composition of the ^{196,198}Pb beams from HIE-ISOLDE, we require **1 shift each isotope** of laser on/off running. To demonstrate the expected low background from fusion-evaporation, we request **3 shifts** with beam on a pure carbon target. A further **1 shift** is required for beam tuning and preparation of the experimental setup.

In summary, a total of **26 shifts** are requested for this experiment. The data will be analysed by a current Liverpool Ph.D. student for their thesis.

References

[1] E. K. Warburton, J. A. Becker, and B. A. Brown, Phys. Rev. C **41**, 1147 (1990).

[2] O. Sorlin and M.-G. Porquet, Prog. Part. Nucl. Phys. **61**, 602 (2008).

[3] A. Poves, J. Phys. G Nucl. Part. Phys. **43**, 024010 (2016).

[4] T. Otsuka, T. Suzuki, R. Fujimoto, H. Grawe, and Y. Akaishi, Phys. Rev. Lett. **95**, 232502 (2005).

[5] Y. Tsunoda, T. Otsuka, N. Shimizu, M. Honma, and Y. Utsuno, Phys. Rev. C **89**, 031301 (2014).

[6] T. Otsuka and Y. Tsunoda, J. Phys. G Nucl. Part. Phys. **43**, 024009 (2016).

[7] B. A. Marsh et al., Nat. Phys. **14**, 1163 (2018).

[8] J. L. Wood, K. Heyde, W. Nazarewicz, M. Huyse, and P. van Duppen, Phys. Rep. **215**, 101 (1992).

[9] K. Heyde and J. L. Wood, Rev. Mod. Phys. **83**, 1467 (2011).

[10] C. Qi, L. Y. Jia, and G. J. Fu, Phys. Rev. C **94**, 014312 (2016).

[11] J. Pakarinen et al., Physical Society of Japan **6**, 020011 (2015).

[12] J. Pakarinen et al., Journal of Physics G: Nuclear and Particle Physics **44** (2017).

[13] R. Julin, K. Helariutta, and M. Muikku, J. Phys. G Nucl. Part. Phys. **27**, R109 (2001).

[14] G. D. Dracoulis et al., Phys. Rev. C **67**, 5 (2003).

[15] R. Julin, T. Grahn, J. Pakarinen, and P. Rahkila, J. Phys. G Nucl. Part. Phys. **43**, 024004 (2016).

[16] J. Ojala et al., Communications Physics **5** (2022).

[17] A. N. Andreyev et al., Nature **405**, 430 (2000).

[18] L. Ducroux et al., Z. Phys. A **356**, 241 (1987).

[19] M. Kaci et al., Z. Phys. A **354**, 267 (1996).

[20] J. Pakarinen et al., Phys. Rev. C **80**, 031303 (2009).

[21] N. Fotiades et al., J. Phys. G Nucl. Part. Phys. **21**, 911 (1995).

[22] R. Bengtsson and W. Nazarewicz, Z. Phys. A **334**, 269 (1989).

[23] J. C. Griffin et al., Nucl. Physics, Sect. A **530**, 401 (1991).

[24] J. Vanhorenbeeck et al., Nuclear Physics A **531**, 63 (1991).

[25] J. L. Wood, E. Zganjar, C. De Coster, and K. Heyde, Nucl. Phys. A **651**, 323 (1999).

[26] K. V. de Vel et al., Phys. Rev. C **65**, 064301 (2002).

[27] K. Wrzosek-Lipska and L. P. Gaffney, J. Phys. G Nucl. Part. Phys. **43**, 024012 (2016).

[28] K. Wrzosek-Lipska et al., Eur. Phys. J. A **55**, 130 (2019).

[29] V. N. Fedoseyev et al., Hyperfine Interactions **127**, 409 (2000).

[30] U. Köster et al., Nuclear Instruments and Methods in Physics Research, Section B: Beam Interactions with Materials and Atoms **204**, 347 (2003).

[31] T. L. Tang et al., Phys. Rev. Lett. **124**, 062502 (2020).

[32] D. K. Sharp et al., CERN-INTC-2021-010 **INTC-P-594** (2021).

[33] O. B. Tarasov and D. Bazin, Nuclear Instruments and Methods in Physics Research, Section B: Beam Interactions with Materials and Atoms **266**, 4657 (2008).

[34] M. Macfarlane and S. Pieper, Ptolemy: a program for heavy-ion direct-reaction calculations, 1978.

[35] A. J. Koning and J. P. Delaroche, Nucl. Phys. A **713**, 231 (2003).

[36] H. An and C. Cai, Phys. Rev. C **73**, 054605 (2006).

[37] A. Matta et al., J. Phys. G Nucl. Part. Phys. **43**, 045113 (2016).

[38] P. T. MacGregor et al., Phys. Rev. C **104**, L051301 (2021).

3 Details for the Technical Advisory Committee

3.1 General information

Describe the setup which will be used for the measurement. If necessary, copy the list for each setup used.

☒ Permanent ISOLDE setup: *ISOLDE Solenoidal Spectrometer*

- ☒ To be used without any modification
- ☐ To be modified: *Short description of required modifications.*

☐ Travelling setup (*Contact the ISOLDE physics coordinator with details.*)

- ☐ Existing setup, used previously at ISOLDE: *Specify name and IS-number(s)*
- ☐ Existing setup, not yet used at ISOLDE: *Short description*
- ☐ New setup: *Short description*

3.2 Beam production

For any inquiries related to this matter, reach out to the target team and/or RILIS (please do not wait until the last minute!). For Letters of Intent focusing on element (or isotope) specific beam development, this section can be filled in more loosely.

- Requested beams:

Isotope	Production yield in focal point of the separator ($/\mu$C)	Minimum required rate at experiment (pps)	$t_{1/2}$
^{196}Pb	2.0×10^7	1.0×10^6	37 m
^{198}Pb	1.8×10^7	1.0×10^6	2.4 h

- Full reference of yield information (*yield database and J. Pakarinen et al., Physical Society of Japan 6, 020011 (2015).*)
- Target - ion source combination:
- RILIS? (*Yes for Pb*)
  - ☐ Special requirements: (*isomer selectivity, LIST, PI-LIST, laser scanning, laser shutter access, etc.*)
- Additional features?
  - ☒ Neutron converter: (*for isotopes 1, 2 but not for isotope 3.*)
  - ☐ Other: (*quartz transfer line, gas leak for molecular beams, prototype target, etc.*)
- Expected contaminants: *Isotopes and yields*
- Acceptable level of contaminants: (*Not sensitive to stable contaminants, limited by ISCOOL overfilling, etc.*)
- Can the experiment accept molecular beams?
- Are there any potential synergies (same element/isotope) with other proposals and

LOIs that you are aware of?

3.3 HIE-ISOLDE

For any inquiries related to this matter, reach out to the ISOLDE machine supervisors (please do not wait until the last minute!).

- HIE ISOLDE Energy: *(MeV/u); (exact energy or acceptable energy range)*
  - ☒ Precise energy determination required
  - ☐ Requires stable beam from REX-EBIS for calibration/setup? *Isotope?*
- REX-EBIS timing
  - ☒ Slow extraction
  - ☐ Other timing requests
- Which beam diagnostics are available in the setup?
- What is the vacuum level achievable in your setup?

3.4 Shift breakdown

The beam request only includes the shifts requiring radioactive beam, but, for practical purposes, an overview of all the shifts is requested here. Don't forget to include:

- Isotopes/isomers for which the yield need to be determined
- Shifts requiring stable beam (indicate which isotopes, if important) for setup, calibration, etc. Also include if stable beam from the REX-EBIS is required.

An example can be found below, please adapt to your needs. Copy the table if the beam time request is split over several runs.

Summary of requested shifts:

With protons	Requested shifts
Yield measurement of isotope 1	
Optimization of experimental setup using 196Pb	1
Data taking, ^{196}Pb	10
Data taking, ^{198}Pb	10
Data taking, ^{196}Pb with carbon target	3
Laser on/off using ^{196}Pb	1
Laser on/off using ^{198}Pb	1
Total	26
Without protons	Requested shifts
Stable beam from REX-EBIS (after run)	
Background measurement	

3.5 Health, Safety and Environmental aspects

3.5.1 Radiation Protection

- If radioactive sources are required:
  - Purpose? Energy calibration of the Liverpool on-axis silicon array using α-source
  - Isotopic composition? ^{148}Gd, ^{239}Pu, ^{241}Am, ^{244}Cm, 4236RP
  - Activity? 1 kBq, 1 kBq, 1 kBq, 1 kBq
  - Sealed/unsealed? Unsealed
- For collections:
  - Number of samples? N/A
  - Activity/atoms implanted per sample? N/A
  - Post-collection activities? N/A

3.5.2 Only for traveling setups

- Design and manufacturing
  - ☐ Consists of standard equipment supplied by a manufacturer
  - ☐ CERN/collaboration responsible for the design and/or manufacturing
- Describe the hazards generated by the experiment:

Domain	Hazards/Hazardous Activities		Description
Mechanical Safety	Pressure	☐	[pressure] [bar], [volume][l]
	Vacuum	☐	
	Machine tools	☐	
	Mechanical energy (moving parts)	☐	
	Hot/Cold surfaces	☐	
Cryogenic Safety	Cryogenic fluid	☐	[fluid] [m3]
Electrical Safety	Electrical equipment and installations	☐	[voltage] [V], [current] [A]
	High Voltage equipment	☐	[voltage] [V]
Chemical Safety	CMR (carcinogens, mutagens and toxic to reproduction)	☐	[fluid], [quantity]
	Toxic/Irritant	☐	[fluid], [quantity]
	Corrosive	☐	[fluid], [quantity]
	Oxidizing	☐	[fluid], [quantity]
	Flammable/Potentially explosive atmospheres	☐	[fluid], [quantity]
	Dangerous for the environment	☐	[fluid], [quantity]
Non-ionizing radiation Safety	Laser	☐	[laser], [class]
	UV light	☐	
	Magnetic field	☒	2.5 T
Workplace	Excessive noise	☐	
	Working outside normal working hours	☐	

	Working at height (climbing platforms, etc.)	☐	
	Outdoor activities	☐	
Fire Safety	Ignition sources	☐	
	Combustible Materials	☐	
	Hot Work (e.g. welding, grinding)	☐	
Other hazards			